



FACULTY OF ENGINEERING AND SUSTAINABLE DEVELOPMENT  
Department of Building Engineering, Energy Systems and Sustainability Science

---

# Quenching a steel plate by water-impinging jets and different simultaneous flow rates

Pablo Martínez Gil

June, 2019

Student thesis, Advanced level (Master degree, one year), 15 HE  
Energy Systems  
Master Programme in Energy Systems

Supervisor: Mohammad Jahedi

Examiner: Mathias Cehlin

---



*A mis padres,  
Emilio y Milagros*



## Preface

This master thesis has been possible thanks to:

My thesis supervisor Mr Mohammad Jahedi, for his support, wisdom and devotion during the development of this study.

My parents, whose love and humility transmitted has made me the brilliant, generous and modest person I am today.

My sister, without whom I had never learnt to hate sitting in the middle seat of the car. Her coping-out mastery always amazed me.

My mates from the Erasmus program, whose reluctance to play Super Smash Bros Brawl on the Wii is still bizarre to me.

My dearest neighbour V, who was capable of inspiring fear on me every time I left my room open.

My best friend Marcos, because one day we will run that pub.

My friends from my city, who after nine months they still cannot tell if I am in Sweden or Switzerland.



## **Abstract**

Regarding the great importance of fast cooling in steel industry for the production processes, a deep understanding of heat transfer and fluid dynamics must be held. A steel plate is heated up until a maximum temperature of 700 °C to be then cooled down seconds later by a configuration of multiple impinging water jets. Different flow rates are used simultaneously by different adjacent jets to perform quenching over the sample, so different hardness is obtained in the material over a small area. Temperature drop in time is measured and monitored by embedded thermocouples and LabVIEW program. To achieve greater understanding of the quenching performance with different flow rates, several parameters are selected to be varied in order to achieve the best working conditions. Jet diameter takes values between 4 and 10 mm, initial temperature of quenching varies from 400 to 700 °C, subcooling temperature is tested for 65 and 75 K, and jet velocity varies between 1.9 and 3.9 m/s. The result of total number of 9 experiments shown that variation of jet diameter does not influence substantially on the cooling rate if flow rate is kept constant. High initial quenching temperature (600-700 °C) led to slightly higher cooling rate in the stagnation region of water jets. The peak value of heat transfer rate in the upwash flow zone was more highlighted for initial quenching temperature 600°C and below it. Higher values of subcooling and jet velocity produce better cooling rates. The result shown higher jet velocity at one column of water jets changes position of upwash flow slightly toward the adjacent column of jets with lower jet velocity. In general, the result shown that all the studied parameters did not have negative effect on obtaining various cooling rates over the steel plate.

## **Keywords**

Quenching, steel, plate, cooling, water-impinging jets, cooling rate, subcooling, temperature.

## Nomenclature

Symbol	Description	Unit
$T_s$	Surface temperature	°C
$T_{sat}$	Saturation temperature of the fluid	°C
$\Delta T_e$	Excess temperature	°C
$q_s''$	Heat flux	W/m <sup>2</sup>
$q_{min}''$	Minimum heat flux	W/m <sup>2</sup>
$q_{max}''$	Maximum heat flux	W/m <sup>2</sup>
$Re$	Reynolds number	-
$H$	Jet-to-surface spacing	mm
$d$	Jet diameter	mm
$A_f$	Open area	mm <sup>2</sup>
$D_h$	Hydrodynamic diameter	mm
$D_h/d$	Open area ratio	-
$\Delta T_{sub}$	Subcooling temperature	K
$T_i$	Initial quenching temperature	°C
$U$	Jet velocity	m/s
$Q$	Flow rate	m <sup>3</sup> /h
$\Delta t$	Frequency of temperature measurement	Hz
$X$	X-axis along the temperature measurement line	mm



# Contents

1. Background.....	1
1.1 Heat treatment process.....	1
1.1.1 Preheating .....	2
1.1.2 Heating.....	2
1.1.3 Quenching.....	3
1.1.4 Annealing.....	7
2. Introduction.....	8
2.1 Quenching techniques .....	8
2.1.1 Water impinging jet.....	8
3. Aims and approach.....	16
4. Experimental method.....	17
4.1 Experimental set-up.....	17
4.2 Experimental procedure .....	20
4.3 Range of parameters .....	20
4.4 List of tests in parametric study.....	22
5. Results and discussion.....	23
5.1 Effect of velocity .....	27
5.2 Effect of jet diameter .....	29
5.3 Effect of initial quenching temperature .....	30
5.4 Effect of subcooling .....	32
6. Conclusions.....	35
6.1 Study results.....	35
6.2 Outlook .....	36
6.3 Perspectives .....	36
7. Index of Figures .....	37
8. Index of Tables .....	39
9. References.....	40



# **1. Background**

Steel, one of the most important materials human race has ever worked with. Throughout history it has been studied and shaped into a large variety of items, pieces and tools. Since the blades and shields antique armies used to fight with, to the very same bridges nowadays we cross, steel has contributed to set the basis of human history.

As years went by, new ways to work this material were discovered, as well as new applications. Sometimes it was even needed to provide steel with new properties to improve its performance under certain working conditions, making it a whole new material with new possibilities. It is one of these property-providing techniques this thesis is mostly interested in, the one called quenching. The process is described as heat treatment, and it consists of heating process, up to temperatures of around 800 - 900°C, followed by fast cooling process. By this technique, the steel piece is hardened and strengthened.

For many years, the steel industry has been aware of this method of enhancing steel, and that is why it has focused on its understanding and development. But despite the deep knowledge scientists have provided, and the new devices created to achieve the proper working conditions, its breakthroughs regarding implementation have not grown at the same rate. Currently, quenching in steel industry is performed following an individual and time-consuming idea, which is based on the idea of sinking the steel into cooling media (bath). Yet, the traditional method is not the only way to achieve quenching, as two other methods are being developed: water jets and water sprays.

But although the main idea may seem pretty clear to the mind, the physics that come along might not be so.

## **1.1 Heat treatment process**

Throughout this process, the microstructure of the steel goes under different states or phases [1]: At first, the microstructure of the material consists of a perlite-grain structure, which is basically a mixture of ferrite and cementite, characterized by its uniformity and laminarity. In fact, the properties of these two different microconstituents which constitute the mixture are completely opposite. Ferrite is known as the softest and most ductile among steel constituents, whereas cementite is the hardest and most fragile.

Once the sample has been heated up and reached the treatment temperature, the microstructure may take two different ways. If the Carbon percentage in the sample is lower than 0.77 %, the microstructure turns completely into austenite. Whereas for those samples with a Carbon percentage higher than 0.77 %, the microstructure turns into a mixture of austenite and cementite. Austenite is characterized by its non-

magnetic properties, as well as being the densest among them all. This current phase is only stable under temperatures over 727°C.

Finally, after the ultra-fast cooling, this microstructure is turned into martensite, having a fine structure. Under these circumstances, Carbon atoms do not have enough time to diffuse, and therefore, cementite cannot be formed. This leads to a carbon oversaturation, which enhances the hardening of the steel sample.

The already mentioned complexity of this technique starts with the heating step. Due to low heat conductivity of steel at low temperatures, this first procedure in the quenching technique must be slow and gradual to avoid fissures and thermal stresses. Extreme care must be taken not to exceed the final heating temperature, since an overheating of the crystalline grain may happen, burning the edges of the grains, and therefore producing oxygen filtration, oxidation, low carbon concentration and excessive fragility of the martensite. So, to avoid all this, the heating step is divided in two processes [2]: preheating and heating.

#### **1.1.1 Preheating**

Steel designed for mechanical construction and tools may find appropriate a preheating up to temperatures of around 400 - 600°C, when initial cooling temperature is less than 900°C. For those with initial cooling temperatures over 900°C, a preheating up to temperatures of around 600 - 700°C may be considered suitable. This first part of the whole heating process must be done meticulously slow.

#### **1.1.2 Heating**

The amount of heating time required to accomplish a right constituent dissolution and a complete austenite state depends on the size and shape of the sample, and its original structure. This heating time encompasses 3 steps:

- Time needed until the piece's surface reaches the temperature of the heater.
- Time needed to transfer heat through the piece until reaching the core and make it to the temperature of the heater.
- Maintenance time needed to accomplish the desired microstructure for the quenching. In other words, it is the time between reaching uniform temperature conditions in the entire piece, and austenite homogenisation.

There are 3 main industrial heaters for this step in quenching: salt bath furnace, continuous furnace and oven box. Each one of them is used depending on the type of quenching is being carried out, and the aim of it.

### 1.1.3 Quenching

The second step in the heat treatment is the cooling process. The range of substances in this process leans on to accomplish its purpose is considerably wide: air, water, mineral oil, molten salts, etc.

Water is the most common cooling substance amongst all, but although it is considerably easy to access to water sources with low cost, it is not considered the ideal one. By itself, water does not show a high level of heat energy removal, due to its low vaporization point. But its properties may be enhanced by adding certain substances that raise this phase change temperature, such as NaCl or NaOH.

Mineral oil is more suitable for low and medium alloy steels, since it can turn austenite into martensite with low cooling velocity value. Besides, the role of mineral oil as cooling substance also reduces internal stresses and quenching shortcomings.

The use of air as cooling substance is related to high alloy steels and complex low and medium alloy steel pieces.

During the cooling process, some points must be ensured in order to perform a correct step [3]:

- High cooling velocity from the final heating temperature until the first transformation of austenite into martensite. The aim of this is to avoid perlite and bainite, and therefore low values of hardness.
- Medium cooling velocity during the transformation of austenite into martensite, which usually happens under 350°C, depending on the material.
- The cooling fluid must not decompose while it is in contact with the heated steel piece.

The first two points from above may be better seen with the help of Figure 1. The blue line shows a cooling rate high enough to transform austenite into martensite only. If the cooling rate value is not high enough to accomplish this, the cooling line will then cross the red curve, and austenite and bainite will be the final constituents. This means the microstructure of the piece might not get the hardness required to carry out its job.

The green curve shows a cooling rate high enough to accomplish the transformations into martensite, with a “pause time” which releases internal stresses. This technique is known as martempering.

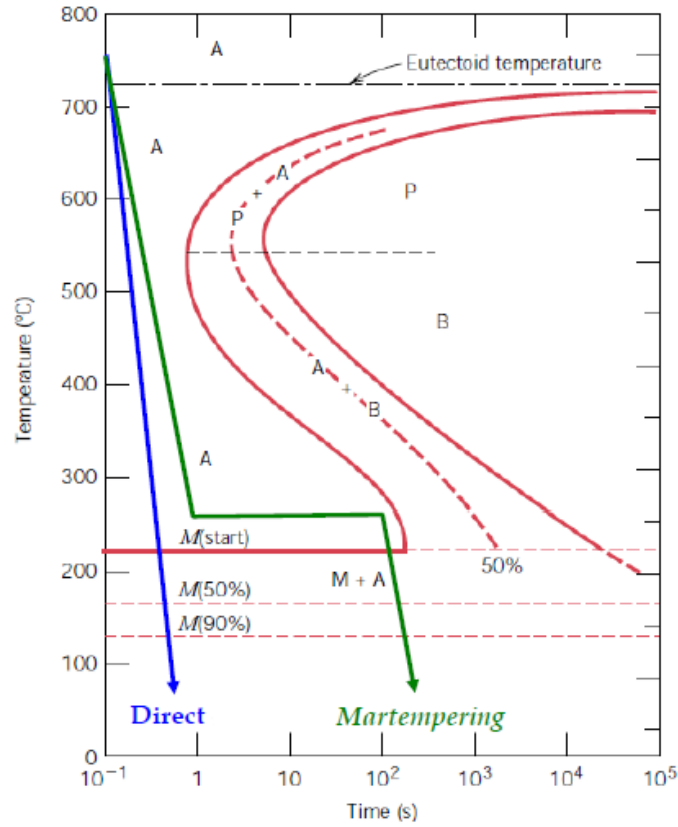


Figure 1: Temperature-time curve during quenching [1].

Regarding the different fluids mentioned above, two groups may be originated in terms of contact with the surface: those which boil, such as water and mineral oil, and those which do not, such as air or molten salts. The latter is characterized by a uniform cooling, while the first group is deemed more complex.

Boiling is defined as a change from liquid to vapor state, and in quenching, it is supported by heat transfer from the surface of the sample. This phenomenon is distinguished by the formation of vapor bubbles, which grow and eventually separate from the sample's surface. The process occurs when the surface temperature,  $T_s$ , is higher than the saturation temperature of the fluid at certain pressure,  $T_{sat}$ . This temperature difference is known as "excess temperature",  $\Delta T_e$ , and its role in the heat transfer phenomenon may be understood by Equation 2.1 [4],

$$q_s'' = h * (T_s - T_{sat}) = h * \Delta T_e \quad (2.1)$$

- $q_s''$ : Heat flux [ $\text{W}/\text{m}^2$ ]
- $h$ : Heat transfer coefficient [ $\text{W}/(\text{K} \cdot \text{m}^2)$ ]
- $\Delta T_e$ : Excess temperature [ $^{\circ}\text{C}$ ]

As said before, this class of fluids which boil with the surface interaction present certain complexity regarding the cooling understanding. Unlike the uniformity of the cooling the other family presents, here it may be seen different regimes or dominions with different characteristics, as cooling rate or temperature.

Figure 2 shows the boiling curve of water at 1 atm, which encompasses 4 different regimes. This graph refers to quenching a thin wire in water bath.

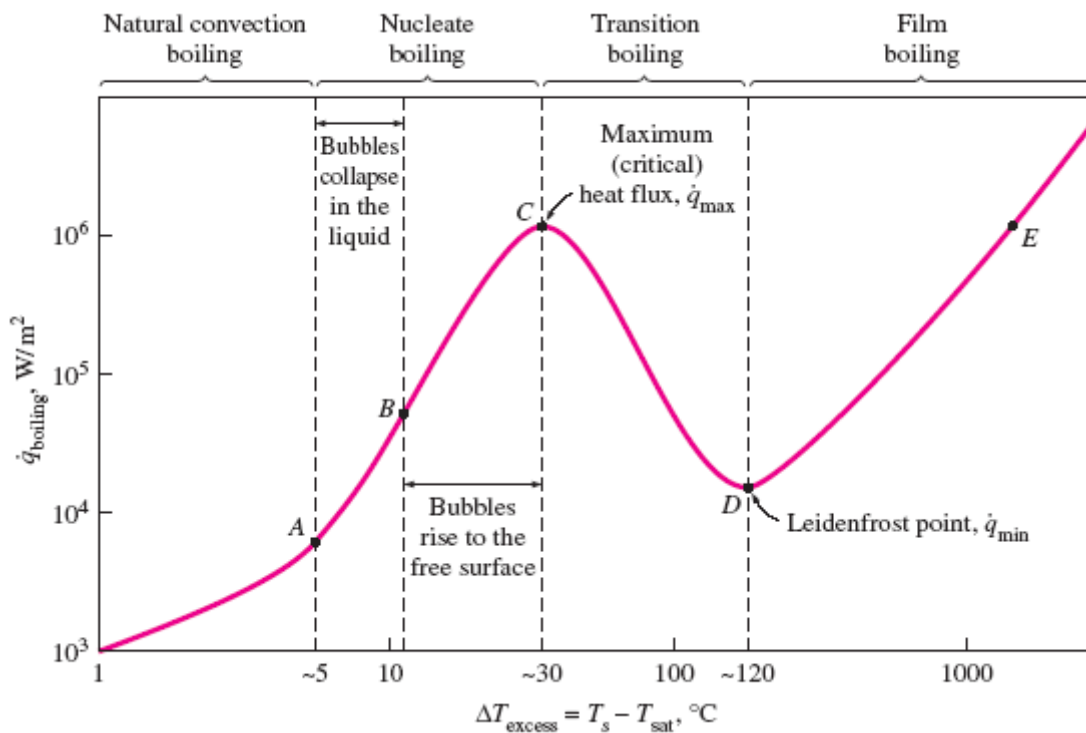


Figure 2: Boiling curve for water at 1 atm [4].

The curve starts its shape since the very first moment the water interacts with the heated surface of the sample, and it keeps being drawn as a positive temperature difference between  $T_s$  and  $T_{\text{sat}}$  exists.

The four different regions that appear should be named as: Film boiling, Transition boiling, Nucleate boiling and Natural convection boiling, or Free convection boiling.

- Film Boiling

This regime begins when water comes into contact with the surface of the sample. At this time, the temperature of the surface  $T_s$  presents a considerably high value,

satisfying  $\Delta T_e \geq \Delta T_{e,D}$  condition for this regime. The first contact between the cooling fluid and the heated piece results in rapid formation of bubbles that form a stable vapor blanket which covers the surface of the steel. This stable vapor layer will keep growing as more water interacts with the surface, reducing the initial cooling rate as the temperature of the surface,  $T_s$ , decreases. Once  $\Delta T_e$  takes the value of around 120 °C, D point is reached, which is commonly referred as the Leidenfrost point. This point does not only mark the border between the film boiling and the transition boiling regime, but presents minimum heat flux value,  $q''_{min}$ .

This regime is characterized by a vapor layer, and it is through it, by conduction and radiation, how heat transfer takes place from the surface to the liquid.

- Transition Boiling

The next region in the boiling curve is the one known as Transition Boiling regime. It has its origin at  $\Delta T_e = \Delta T_{e,D} \approx 120$  °C, and finishes at  $\Delta T_e = \Delta T_{e,C} \approx 30$  °C ( $\Delta T_{e,C} \leq \Delta T_e \leq \Delta T_{e,D}$ ). In fact, this region is considered a transition path between two main regions, Film boiling and Nucleate boiling, so its conditions vary between them.

As  $\Delta T_e$  decreases, the vapor layer thickness is reduced and becomes unstable, prioritising contact between liquid and solid surface. The liquid is known for having higher thermal conductivity than the vapor, so the less vapor surrounds the surface, and the more amount of liquid interacts with solid surface, the higher heat flux,  $q''_s$ . According to

Figure 2,  $q''_s$  grows until reaching its peak value at  $\Delta T_e = \Delta T_{e,C} \approx 30$  °C. Under this temperature, the heat flux turns into maximum value  $q''_{max}$ .

- Nucleate Boiling

Following Transition boiling, Nucleate boiling regimes makes its first appearance just below  $\Delta T_e = \Delta T_{e,C} \approx 30$  °C. Its range goes from this particular point until  $\Delta T_e = \Delta T_{e,A} \approx 5$  °C, and its trajectory may be divided in two subregions, both of them with downward trend.

C point was stated as the one where the maximum heat flux takes place. This means that, under these circumstances, the layer formed since the first contact has been reduced substantially, but the remaining vapor covering the surface does not allow heat flux to keep growing.

The first subregion,  $\overline{CB}$ , is characterized by having much vapor formed again, thus reducing the heat flux as  $\Delta T_e$  decreases. Unlike the vapor from the Film boiling regime, this one does not stick to the surface of the piece, but it rises to the free surface in form of columns.

In the second subregion,  $\overline{BA}$ , the vapor bubbles get more and more closer to the surface of the sample. This leads to a more intense interference between the vapor bubbles, retraining the motion of fluid near the surface, thus reducing  $q''_s$  and  $h$ .



- Free Convection Boiling

The last region within the boiling curve is called Free convection boiling regime. It exists under condition of  $\Delta T_e \leq \Delta T_{e,A} \approx 5^\circ\text{C}$ , but it is important that  $\Delta T_e$  remains positive so boiling can occur. As its name implies, this regime is governed by free convection between the fluid and surface. In this last region, heat flux also reduces as  $\Delta T_e$  decreases, but its trend is not as steep as it was before. Once  $\Delta T_e$  becomes 0, no boiling occurs during the fluid-solid interaction, and cooling becomes uniform from this point on, reducing gradually the heat flux.

All in all, a phase change of the cooling fluid may present some difficulties in the understanding of this phenomenon, but the heat transfer coefficients achieved along these boiling regimes are much higher than the ones achieved with convection with no phase change. This means that higher heat flux values are reached, and therefore better cooling rates for quenching.

Despite the fact this curve is based on quenching by water, similar trends appear with other fluids.

#### 1.1.4 Annealing

Once these two main steps are accomplished, heating and cooling, it is stated that quenching has come to an end. But despite the high fragility the quenched steel shows, and the internal stresses originated by the volume changes of the martensite microstructure, the steel piece needs to undergo another heat treatment process, the so-called annealing. The aim of this technique is to reduce the high fragility of the sample produced by the quenching, despite reducing simultaneously its hardness. To do so, the steel piece is heated up to a temperature lower than the austenization temperature, is kept for a short time, and then cooling process is carried out up to room temperature.

Although this last process has many intel it is possible to dive in, it does not represent a priority for this thesis, so it will be kept aside.

## 2. Introduction

### 2.1 Quenching techniques

As for the different ways to carry out the cooling step, the most known and established pieces of equipment are the water bath, sprays and impinging jets. The first one could be stated as the traditional method, leaving the latter ones as developing systems. The steel industry has used the water bath as its main quenching device for many decades, even nowadays it is used to perform this ultra-fast cooling role (Figure 3).



Figure 3: Industrial water tank used for quenching [5]

But despite its popularity, the setbacks the factories encounter, such as not having good control over cooling process, slowness or chain production interruption bring up the need of looking for alternatives. This thesis is focused on the study of one of these new cooling techniques, the water impinging jets.

#### 2.1.1 Water impinging jet

According to Weigand and Spring [6], jet impingement systems provide an effective means for the enhancement of convective processes due to the high heat and mass transfer rates that can be achieved.

An impinging jet is basically a cylindrical tool, of certain area, through which water, or any other fluid, may be forced to flow with certain velocity (Figure 4).

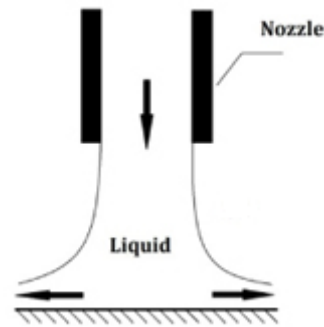


Figure 4: Jet impinging jet [6]

Depending on the number of impinging jets used for the configuration, they may be classified as: single jet or multi-jet configuration. The differences between them lie not only in the number, but in the flow and heat transfer as well. The reason of this is that, under certain conditions, the flow coming from a jet may interact with the flow of an adjacent jet. The point where this interaction takes place originates two different types of interference:

- Jet to jet interference before impingement on the surface (in case of small jet-to-jet spacing).
- Interaction among the surface flows (wall jets).

With only taking this into account, it is easy to see how working with single jet configurations brings fewer problems than multi-jet configuration. The design of the latter regarding heat transfer is described as a tedious and complex work, since many variables get involved. On the other hand, and being a common point for both single and multi-jet design, the settled flow and geometrical parameters need to provide both an efficient and uniform heat transfer over the surface of the piece.

Being the flow and heat transfer the two main characteristics of this method, special attention should be paid on their comprehension.

#### 2.1.1.1 Fluid flow

The complexity of this characteristic lies on its evolution since the very first moment it leaves the nozzle until it spreads along the surface. This fluid development is usually found divided in three different regions [6]: the free jet region, the stagnation flow region, and the wall jet region.

For a better understanding and visualization, Figure 5 shows this division for a single impinging jet.

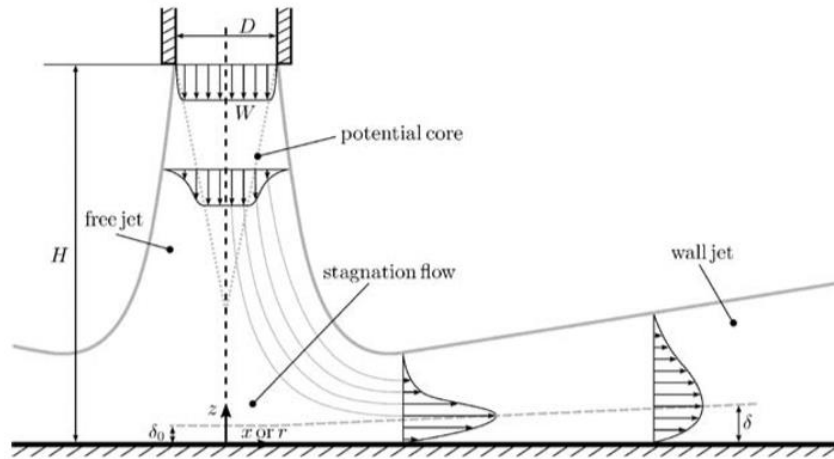


Figure 5: Fluid flow regions of a single impinging jet [6]

The first division is the free jet region. Inside it, the fluid flow starts to broaden more and more, due to it is no longer confined. As this happens, the potential core, i.e., the area where the flow velocity still has the same value as the bulk jet velocity at the nozzle exit,  $W$ , becomes narrower and narrower, until it finally disappears, losing this maximum velocity value. Obviously, this kinetic energy from the axial velocity component cannot just vanish, but it generates an acceleration on the horizontal plane. Once the flow reaches the surface, the free jet region ends, and the stagnation flow region begins. This division just covers an area not much bigger than the stagnation point, being intensely affected by the wall itself.

The last region is called wall jet region, and it encompasses the radial spread of the flow after its encounter with the surface. In terms of horizontal velocity, the flow presents a value of zero at the stagnation point, so in this region it is accelerated until reaching a maximum value at certain distance, which has the value of about one jet diameter from the stagnation point [6].

Despite being this content aimed at a single impinging jet, the flow of a multi-jet configuration presents the same divisions, although some crucial differences may show up.

The first one could be the possibility of an interaction between adjacent fluid jets before reaching the surface of the sample. This is the result of an excess of fluid flow expansion in the free jet region, either by a small separation among the jets, or a small distance between the nozzle and the stagnation point.

Another difference may lie on an interaction between wall jets after the impingement takes place. The flows originated at the stagnation points over the surface interact with each other, creating upwash flows or fountains (Figure 6). The size of the fountain depends on jet-to-jet spacing, jet-to-surface distance and a high fluid jet velocity.

As one may realize, these two events are based on the two interferences mentioned at the beginning of this chapter.

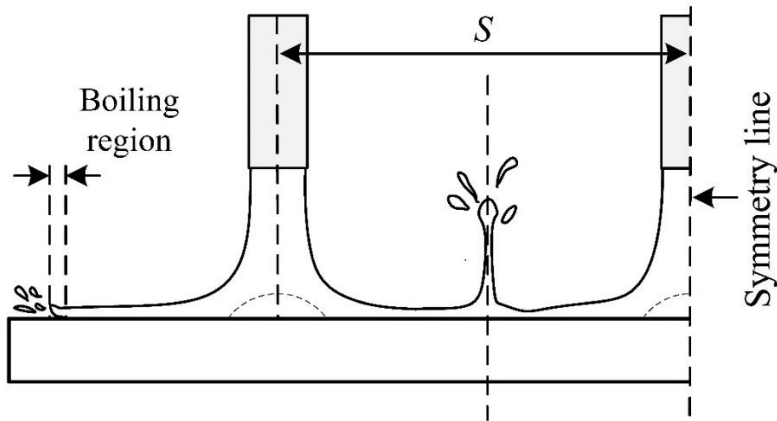


Figure 6: Possible fountains developed in a multi-jet configuration [7]

#### 2.1.1.2 Heat transfer

Heat transfer is the basis of what researchers and scientist are trying to achieve in this whole field. The main goal is to reach high cooling rate values by the use of water impinging jets, so cooling may take place at shorter time. The boiling phenomenon is not similar to quenching steel in water bath, although some boiling regimes are introduced during the quenching process.

Some studies, such as the one performed by Hatta et al. [8], achieved major breakthroughs on their attempt to understand the heat flux distribution during the process. They conducted an experiment on quenching a steel plate by subcooled water jet, and during the tests it was possible to observe three different cooling regions created over the surface: The wetted region, the annular region and the unwetted region. The results of the tests showed that the highest heat flux value took place within the wetted region, specifically next to the stagnation point. It was possible to observe that this region was governed by nucleate boiling, although more and more transition boiling conditions were adopted as observations moved away from the stagnation point. On the other hand, the annular region was defined as an area where transition boiling happened, and fluid was removed from the surface by drops due to resistance of large temperature difference between fluid and solid, which avoids the fluid to keep spreading and quenching the piece. This phenomenon had its reason on the vapor bubbles created on the first contact between the fluid and the heated surface, which spread radially until gathering at certain distance, creating a film that isolated the surface from the water [9]. Finally, the furthest region from the stagnation point was identified as been ruled by film boiling, since the water drops spread away over the vapor layer. Karwa et al. [10] determined that this fluid-solid contact over the surface does not take place until the fluid is strong enough to eliminate the vapor layer, so the wetted region can expand radially. In their experiment they concluded that increasing parameters such as jet velocity or subcooling results in a higher propagation velocity of the wetted region, wetting front velocity, could be obtained, though this value reduced as moving away from the stagnation point. This idea was based on the observation of

getting smaller vapor bubbles in the regions under these circumstances, which originated a weaker resistance to the fluid flow. This allowed the wetting front to grow in a bigger rate, achieving both more uniform and higher cooling rates. Figure 7 shows the different regions established on the impingement surface during quenching.

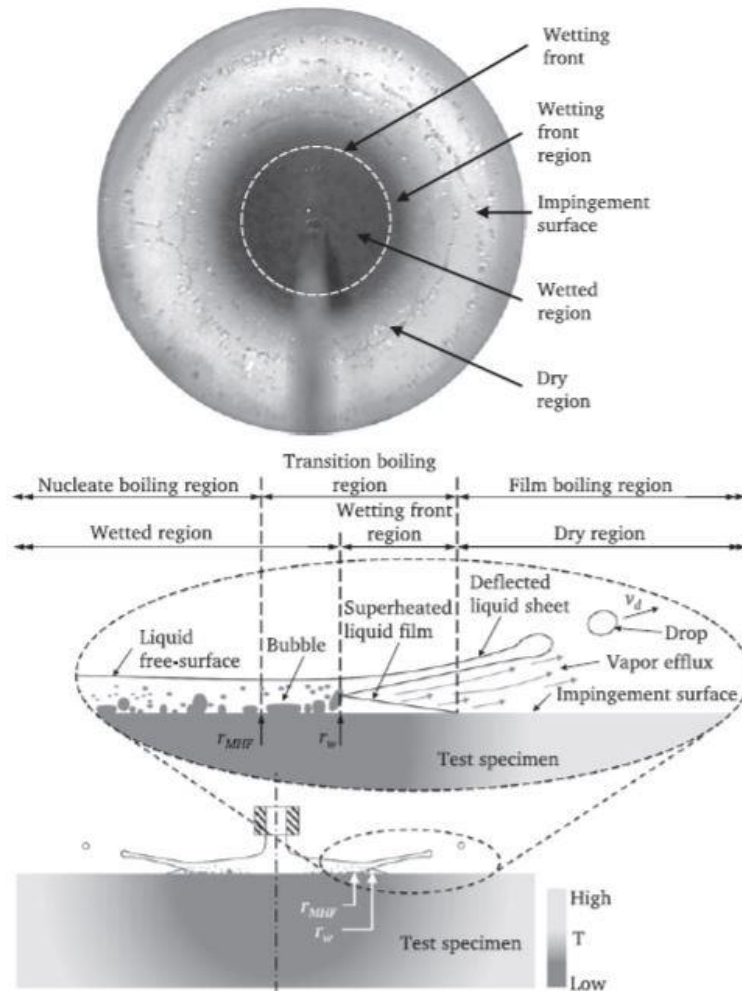


Figure 7: Distinct regions identified on the impingement surface during quenching [10]

Unfortunately, heat transfer phenomenon is not something which can be easily controlled, and its performance is affected by several parameters, such as: bulk jet velocity at the nozzle exit, nozzle shape, initial temperature of surface, jet-to-jet spacing, fluid flow development over the surface, turbulence level, etc.

All these variables are not independent from each other, but they are interconnected. This undoubtedly makes the study more complex, since the one same parameter should be studied from other variables' point of view.

Although fluid flow and heat transfer have been presented as two different phenomena, truth is there exists a profound relationship between them. All the variables mentioned

above are linked to heat transfer by the fluid flow. They all set the basis to achieve a final cooling rate value, but it is by the fluid performance the way variables' effects are not only taken into consideration, but also comprehended.

#### **2.1.1.3 Quenching parameters by water impinging jet**

Despite the numerous influencing factors or variables which affect heat transfer in this process, this thesis only focuses on a few of them:

- Jet velocity

Jet velocity, or bulk jet velocity, is a parameter which measures the speed the water possesses when leaving the nozzle. Its role is considered decisive in the quenching process, and therefore many researchers have carried out a good deal of experiments to unravel it completely. Jahedi et al [11]. performed an experiment on a rotating hollow cylinder by one row of water impinging jets. Along its development, it could be seen that low values of Reynolds number ( $Re = 8,006$ ) reported low cooling rates, whereas higher jet velocities ( $Re > 8,006$ ) resulted in more extreme temperature drops above 400 °C, thus higher cooling rates. They concluded that higher  $Re$  values brings better liquid-solid contact in film and transition boiling, but it is meaningless in nucleate boiling.

- Jet-to-surface spacing

It is defined as space between the nozzles and surface of quenching specimen. This variable is represented by dimensionless number  $H/d$ , with  $H$  equal to the straight distance from the nozzle exist to the surface, and  $d$  as the nozzle diameter. Its importance lies mainly in multi-jet configurations, and it is due to the possible interaction among the water jets before reaching the impinging point on the surface, a phenomenon which does not occur when working with single-jet configurations. As stated before, these interferences report low heat transfer values, so many experiments have been performed in order to designate which separations distance ranges should be avoided, and which should be considered appropriate. Xiaojun et al. [12] carried out several tests on quenching a flat plate with an obliquely impinging circular air jet, and they established that this interference becomes more and more intense as  $H/d$  increased, weakening the jet, and therefore degrading the heat transfer phenomenon. The optimum range of  $H/d$  was set up between 6 and 8 times the  $d$  value. This idea was subsequently extended with experiments that determined that this jet-to-surface distance effect was negligible for flows with small Reynolds number [7].

- Open area ratio

The parameter “*open area*”,  $A_f$ , is defined as cooling area corresponding to each individual impinging jet. The relative hydrodynamic diameter,  $D_h$ , of surface area covered by each jet is calculated as follow:

$$D_h = \sqrt{\frac{4 * A_f}{\pi}} \quad (2.2)$$

The *open area* ratio,  $D_h/d$ , between the internal diameter of the nozzle ( $d$ ) and the hydrodynamic diameter of surface area covered by the jet ( $D_h$ ), is defined as dimensionless parameter related to size of impinging jet and the cooling area. This relation must be treated carefully, since heat transfer is deeply affected by its development. Throughout the last past years, several experiments and researches have proven a relationship between the *open area* parameter and the jet-to-jet spacing factor [7], [13]. The reason of this was determined when analysing the heat transfer’s ongoing for very small values of  $A_f$ , which, for multi-jet configurations, corresponded to big jet-to-jet spacing configurations. Since those points where heat transfer peaks take place, stagnation points, are far from each other, the surface is not properly covered by these key points for a fast cooling. Conversely, if  $A_f$  is given too high values, the jets interacted with each other after the impingement, degrading the heat transfer phenomenon. Therefore, it was stated that medium values of  $A_f$  should be taken in order to get suitable heat transfer values and uniformity [6].

- Subcooling temperature

This term is referred to the temperature of cooling fluid which is lower than the saturation temperature of fluid at certain pressure,  $T_{sat}$ . It is expressed by  $\Delta T_{sub}$ , which represents the difference between  $T_{sat}$  and fluid temperature. Jahedi et al. [7] performed several experiments focusing on how effect of this factor could be to the heat transfer phenomenon. They concluded for their experiment that with medium values of  $\Delta T_{sub}$ ,  $55 \leq \Delta T_{sub} \leq 65$  K, the cooling trends were similar, and no difference was shown. Yet, when  $\Delta T_{sub}$  was forced to reach higher values, of around 80 K, an enhancement in the cooling rate occurred in both the film and transition boiling regime. Gradeck et al. [14] had previously carried out similar experiments, and in their research, a solid attempt to understand the development of the Leidenfrost temperature was made. They found that this Leidenfrost temperature increases with subcooling, allowing the transition boiling regime to last longer, and therefore reaching a higher maximum heat flux,  $q''_{max}$ . Islam et al. [15] experimented with heated cylindrical steel pieces and impinging water jets, working within a range of  $5 \leq \Delta T_{sub} \leq 50$  K, and in the resulting temperature-time curves, it could be seen that the higher the jet velocity and the subcooling, the lower the time to perform quenching.



- Initial quenching temperature

The initial quenching temperature,  $T_i$ , establishes which boiling regime the cooling process starts with over the surface. Jahedi and Moshfegh [10, 12], have studied this parameter in several of their experiments, trying to comprehend its nature. In one of their studies, they decided to work with an initial surface temperature range of 250-600 °C, and their results showed that working with  $T_i$  as close as possible to the Leidenfrost temperature brings up higher  $q''_{max}$ . Quenching with rather high values of  $T_i$ , 550-600 °C for the experiment, resulted in lower values of heat transfer along different regimes, mostly by the thicker vapor layer generated at the film boiling regime. Besides,  $T_i > 600$  °C would also mean longer time to reach  $q''_{max}$  point. On the other hand, working with really low initial surface temperatures, below the maximum heat flux point, would not allow to achieve  $q''_{max}$ .

The experiments also showed that the cooling rate values within the nucleate boiling regime were practically independent from  $T_i$ , so this temperature's influence was located upwards. In conclusion, working with in-between  $T_i$  values, transition boiling regime, provides not only better cooling rates, but also less time to reach  $q''_{max}$ . According to the results,  $T_i = 350$  °C delivered the highest heat transfer value under the surface, and the shortest time to meet the peak value.

Summarizing, many has been discovered during the past years about the nature of this technique. The studies, the experiments and the reviews performed by scientists and researchers have contributed to comprehend quenching in ways never imagined. The physics, the engineering, even new potential applications of this technique move forward with every passing day. But despite all these breakthroughs and tenets developed throughout the years, many fields remain unknown. Multi-jet configurations, simultaneous different cooling flow rates performance and other concepts and techniques await to be studied and understood. Thus, the author of this master thesis committed himself to contribute to this quest by carrying out some experiments to help understand some of these ignored aspects.

### **3. Aims and approach**

So far it has been presented everything that was achieved and understood about quenching throughout the years by the performance of multiple experiments and tests. But now the question is: What comes next? Where does this whole path lead to? What is the next step to take? During the previous chapters some clues have been given about which direction this thesis is going under, which fields are left aside, and which theories and ideas will be used as means of support.

The main goal of this master thesis is study of quenching by water impinging jets on a heated plate. The research will deep into analysing the role of multi-jet configurations, by providing simultaneously different flow rates during the quenching in the neighbour jets, which will correspond to obtain different material properties in a small open area. In another word, the main focus of this study is to investigate if large differences of cooling rate over small quenching area can be obtained by applying two different flow rates on the adjacent jets, which can lead to obtaining different material properties in different parts of small steel sample for specific practical purposes. These aims will be addressed by acting on some influencing parameters, such as jet velocity, open area ratio, subcooling temperature and initial surface temperature. Many experiments have been performed developing numerous patterns and criterions on how these and many other factors behave respecting heat transfer, but never under these specific experimental conditions. A priori, it is not expected to find contradictory evidences regarding previous conclusions and statements, but there lies the possibility of developing a deeper understanding on certain areas that may help to adjust and refine the preceding approaches.

This study will not only shed some light into the multi-jet configuration comprehension, but also in the pursuit of better cooling rates and how to accomplish them.



time. The water used for quenching is delivered by the water tank placed on top, and the returning water from the chamber is pumped into a second tank placed below. Two-way solenoid valves are used to control the direction of the water flow towards the chamber, whereas some other valves are used to control the flow within the recirculating line.

As for where the sample is placed, and therefore the heating and cooling takes place, the chamber takes that role. It is in essence a metal empty box with enough space to take in the sample plate. On one wall there is a vertical hatch through which the heater can enter and exit, whereas the other one has an adaptor to attach the plate to the servomotor, so it can rotate during the heating step to heat up more uniform before quenching and stay put during the cooling process. To avoid cooling the other sides of the plate, insulation is set over them, fixed by four rectangular support plates screwed to the sample plate. Regarding the jets, a total number of eight nozzles constitute the whole configuration. The jets are divided in two groups, one group fed by one pump, and the other group fed by the other pump. Since it is desired to work with different flow rates simultaneously, four water jets are connected to the first pump, and the other four water jets to the second one. The chamber's ceiling is where the jets are located aiming the plate, and the floor has a drainage to take away the water used for cooling. More detail of cooling configuration may be seen in Figure 9.

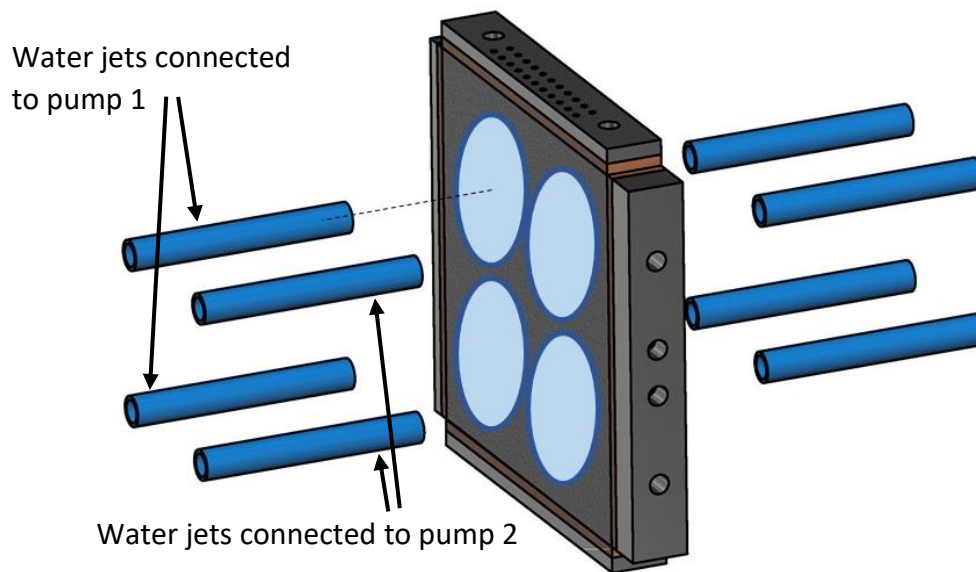


Figure 9: Schematic of nozzles and plate

To record data during the experiment, 22 N-type thermocouples ( $\varnothing$ -0.75mm) are placed in two depths inside the plate, so measurement signal of the temperature during both the heating and cooling processes is collected (Figure 10). All this intel is stored in a

Labview software, which can lately be exported to an Excel file. The thermocouples are lined up longitudinally in two rows, 11 sensors each. The thermocouple line closer to the surface and the one placed in the middle are named as  $R_2$  and  $R_1$  respectively. The distances between the sensors are 5 mm longitudinally and 4.5 mm transversally, with the line set to start 25 mm away from the ends. More details regarding the experimental configuration and the process may be found in the study of Jahedi and Moshfegh [7].

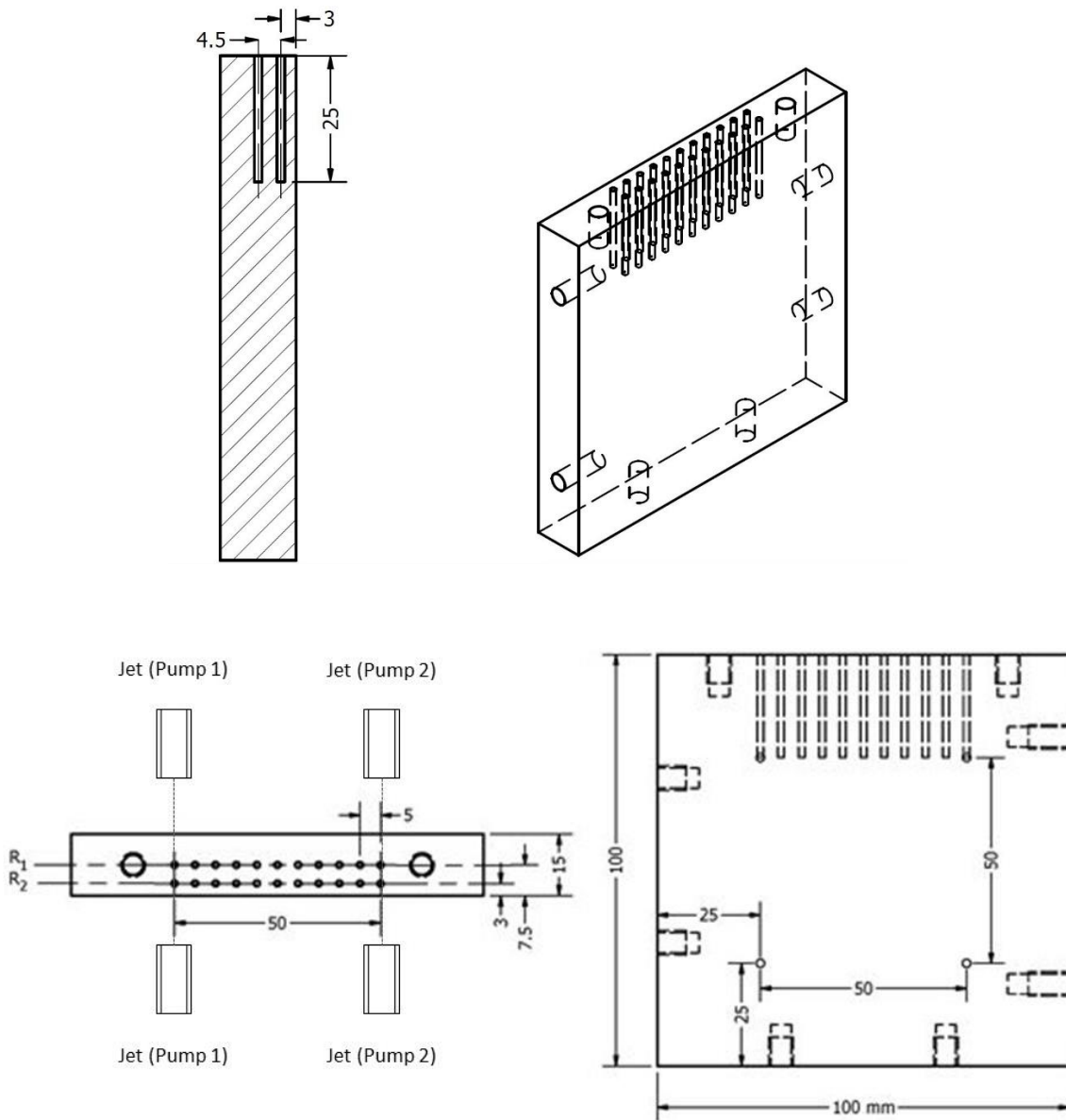


Figure 10: Schematic of jet position and the drilled configuration of holes in the plate to install thermocouples in lines  $R_1$  and  $R_2$ .

## 4.2 Experimental procedure

The process to perform the test goes as follows:

1. Initial considerations and checks must be performed: The sample is put in position, the valves are open, so the water can flow in the internal circulation, the flow rate is checked by the flow meter, and the input values of initial and final quenching temperatures and servo motor rotating speed are set.
2. The servo motor is switched on and the induction heater is placed inside the chamber, keeping the sample plate inside.
3. The heating step starts, and it goes until the test temperature has been reached. The heating is done up to slightly upper than the initial quenching temperature. The temperature evolution is followed thanks to the thermocouples placed inside the plate, which collect and send the data to the Labview program in the computer. There it is possible to track down not only the temperature of the measuring points, but the mean temperature of the whole plate too.
4. Once the heating step has been accomplished, and a temperature uniformity can be appreciated, the servo motor is stopped, the heater is removed quickly from the chamber, the hatch is closed, and the water impinging jets are placed in position, sealing the whole chamber. All in all, the water chamber is completely shut for the cooling step.
5. Now, as soon as initial quenching temperature is obtained, the quenching is set in motion, and the water jets starts to cool down the plate. Pump 1 is activated automatically, whereas pump 2 needs a manual opening process on its following valve. The thermocouples keep measuring the temperature variation, and a temperature-time curve is created.
6. The cooling process stops once the input final temperature value has been reached by the mean temperature of the plate. No more data is recorded, and the experiment is finished.

## 4.3 Range of parameters

The sample used for the experiments is a 100 x 100 x 15 mm carbon plate. Along the study it is tested under different conditions, varying one parameter at a time, while the rest are kept under their reference value. Previously, it had been mentioned that two different flow rates are used simultaneously to perform quenching, and therefore the water jets need to connect to separate water pumps. That said, only the jets and the flow rate related to pump 1 are meant to suffer variations from their reference values, whilst the jets and rate of pump 2 suffer none.

Table 1 shows the different parameters tested during the experiments, as well as the units and values they take. As it may be clear to the eye, open area ratio,  $D_h/d$ , is constituted by two parameters, and whereas  $D_h$  keeps a constant value of 112.8 mm,  $d$  may be 4, 6 and 8 mm. Parameter  $H$  refers to the jet-to-surface spacing, and along with  $Q_{pump2}$  and  $d_2$ , being the latter the diameter of the jets connected to pump 2, they are kept constant during the study. These constant values are defined as reference values, and in

Table 1 they are shown in bold.

Table 1: Designed range of parameters in the experiments.

Parameter	Unit	Range
$U$	m/s	<b>1.95</b> , 2.9, 3.9
$\Delta T_{sub}$	K	65, <b>75</b>
$T_i$	°C	400, 500, 600, <b>700</b>
$D_h/d$	-	28.2, <b>18.8</b> , 14.1
$H$	mm	<b>2</b>
$Q_{pump2}$	m <sup>3</sup> /h	<b>0.45</b>
$d_2$	mm	<b>6</b>
$U_2$	m/s	<b>1.10</b>

The heating step starts with the sample at room temperature, and it goes up to 730 °C. From this point, the cooling step works under a temperature range of 700-100 °C. Since several thermocouples are used to measure the temperature of different points along the whole process, it has been decided to use mean values of all measured temperatures as reference value of initial temperature. Within this temperature range, maximum uncertainty of thermocouple sensor takes place in 600 °C at level of  $\pm 0.9\%$ . The uncertainty of sensor location, water temperature and water flow rate are  $\pm 4.6$ ,  $\pm 9.2$  and  $\pm 0.7\%$  respectively, with an estimate level of confidence of 95%. Regarding thermal conductivity, heat capacity and density of steel, mean values are considered: 51 W/m.K, 470 J/Kg K and 7.8 g/cm<sup>3</sup> respectively. On the other hand, the chemical composition of the sample plate is described in Table 2.

Table 2: Material concentration of the sample [16].

C [%]	Si [%]	Mn [%]	S [%]	P [%]	Cr [%]	B [%]
-------	--------	--------	-------	-------	--------	-------

<b>Min</b>	0.25	0.1	1.1	0.01	0.02	0.2	0.0008
<b>Max</b>	0.3	0.4	1.3	0.01	0.02	0.5	0.005

#### 4.4 List of tests in parametric study

The different tests performed in this parametric study are listed in Table 3. With the exception of Test 1, in which all the parameters take their reference values, the rest have experienced the variation of one parameter to analyse its effect upon quenching. As it may be seen, a total number of 9 different tests have been performed, and for each one of them, different results have been reported. Test 1 is defined as the “reference test”, Test 2 and 3 focus on the analysis of jet diameter effect, Test 4 and 5 on jet velocity effect, Test 6, 7 and 8 on the initial temperature effect, and Test 9 on subcooling effect. Due to the difficulty of achieving the right conditions to perform tests aimed to analyse this last effect, only one experiment of these characteristics, apart from the reference test, has been possible.

Table 3: List of tests in the parametric study.

	$U$	$\Delta T_{sub}$	$D_h/d$	$T_i$
<i>Test 1</i>	1.9	75	18.8	700
<i>Test 2</i>	1.9	75	28.2	700
<i>Test 3</i>	1.9	75	14.1	700
<i>Test 4</i>	2.9	75	18.8	700
<i>Test 5</i>	3.9	75	18.8	700
<i>Test 6</i>	1.9	75	18.8	400
<i>Test 7</i>	1.9	75	18.8	500
<i>Test 8</i>	1.9	75	18.8	600
<i>Test 9</i>	1.9	65	18.8	700



## 5. Results and discussion

The results obtained from the experiments are collected thanks to the thermocouples set in the plate, which track the temperature of different points along the whole test. As mentioned before, 22 of these sensors constitute the information caption system, and each one of them report the temperature development of a specific point during quenching. Figure 10 provided an insight on how the thermocouples are set along the plate. It could be seen that 2 lines were formed longitudinally, one in the middle ( $R_1$ ) and one close to the front side ( $R_2$ ). Since the plate is cooled down from the bigger sides, the temperature evolution of the points closer to the surface will not be equal to the one of the points centred. This leads to a separate analysis of the thermocouple lines, as it is shown in Figure 11 and Figure 12. These two graphs have been extracted from the results of Test 5.

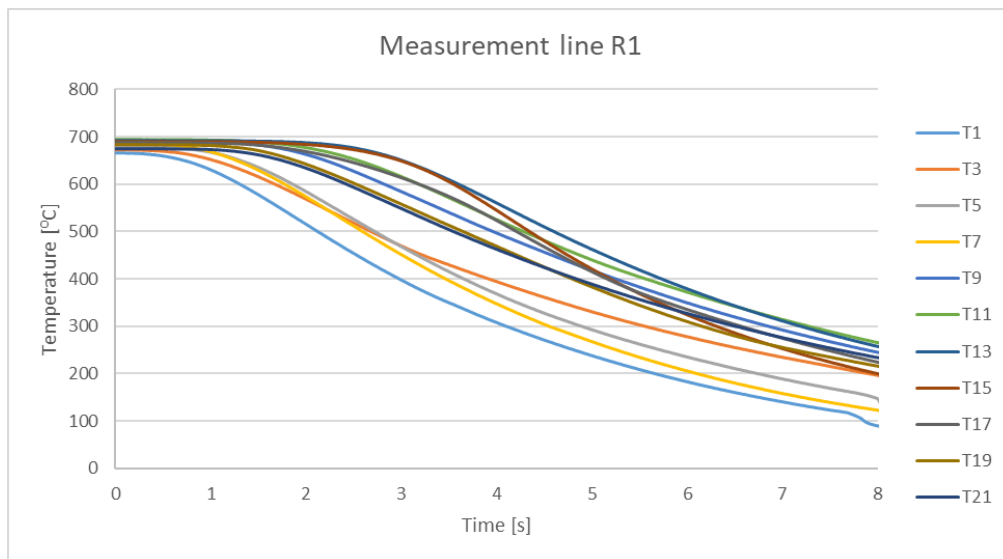


Figure 11: Temperature-time relation of measurement line  $R_1$ , Test 5

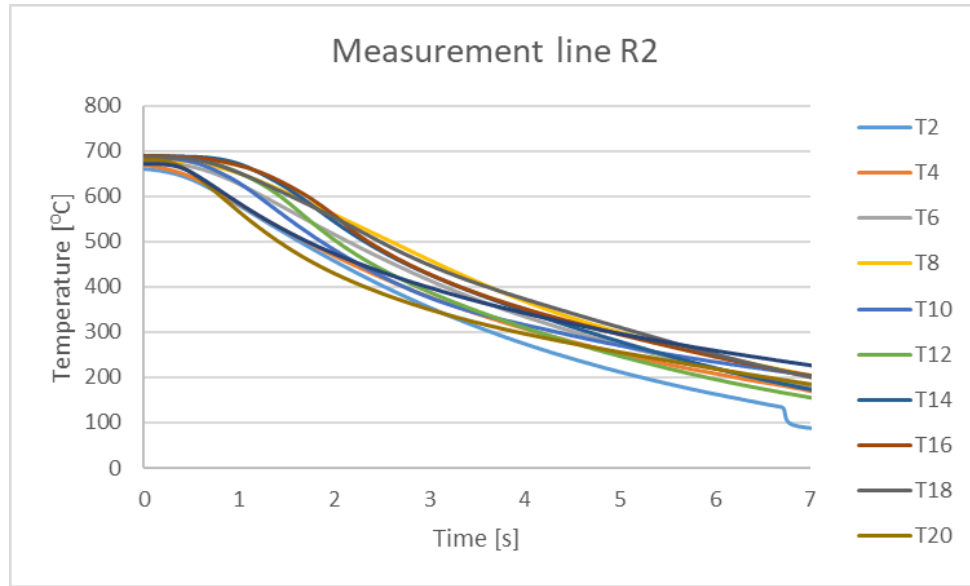


Figure 12: Temperature-time relation of measurement line  $R_2$ , Test 5

The reason of this is that the thermocouples closer to the surface ( $R_2$ ) experience larger temperature drop prior than the ones in the middle row ( $R_1$ ), since heat transfer by internal heat conduction across the plate thickness is not instantaneous. This means that the temperature-time relation shape of the latter will not be as pronounced as the others, due to it takes more time to reach  $R_1$  points. As one may notice in the graphs, the thermocouples placed in the centre of the plate show a slower evolution than the ones of the ends. The reason of this is that they are not within the stagnation area, and thus the cooling is not immediate.

But despite the alleged disadvantages of this separate analysis, the possibility of a temperature tracking along the plate gives information which cannot be dismissed out of hand. Figure 13 and Figure 14 show temperature distribution along  $R_1$  and  $R_2$  measuring line for different times of the quenching process. The x-axis refers to the length of the thermocouple line, being the water jets placed on both ends of it ( $x = 0$  and 50 mm). Theoretically, these two incident points report the highest temperature drop of all, since it is where the highest heat extraction takes place. Meanwhile, the upwash flow point, which somehow is supposed to be found in the middle of the line, should show the lowest temperature drop in the beginning of quenching until upwash flows collide to each other.

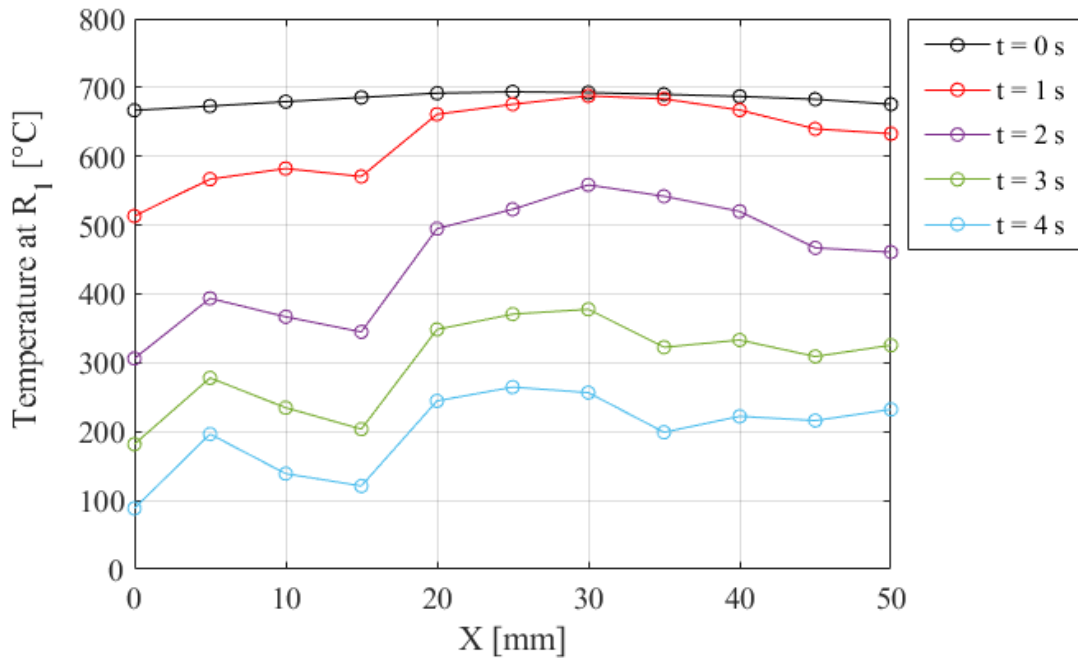


Figure 13: Temperature distribution in line  $R_1$  at different time steps, Test 5

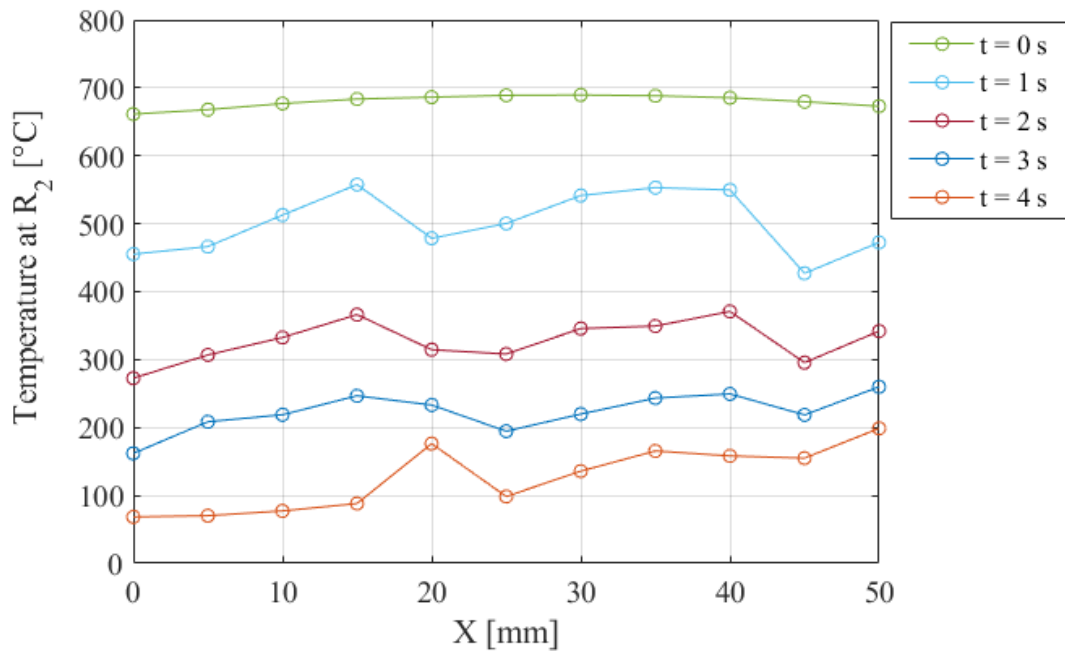


Figure 14: Temperature distribution in line  $R_2$  at different time steps, Test 5

If special attention is paid to the graphs, one may notice that neither the right end shows one of the highest temperature drops, nor the highest point is in the middle. An explanation of this may be found upon the test parameters values given for this experiment in particular. It is highly recommended to recall that whereas the right cooling jets always keep the same quenching conditions, the ones set on the left suffer variations on their parameters. This means that sometimes these jets possess higher

quenching effect than the others, accomplishing bigger heat extractions upon their hydrodynamic area. If these happens, the thermocouples will report higher values of temperature drop on the left side than the ones on the right. Moreover, since  $Q_{pump1}$  used for the test is higher than  $Q_{pump2}$ , which is constant in all the experiments, the strength of the first will push the upwash flow point to the right.

The information presented above comes from Test 5, in which  $Q_{pump1}$  of  $1.6 \text{ m}^3/\text{h}$  is used to quench the left part of the plate. The results of this experiment clearly show how the left end presents the lowest value of temperature (stagnation point), as well as the shifting of the upwash flow point to the right. Figure 13 shows higher temperature in the measuring points along the plate for a certain time than the ones in the Figure 14 for the same time step. This is because line  $R_2$  is closer to the surface, and therefore heat extraction phenomenon is more dominant. Besides, the effect of different flow rates is captured strongly in Figure 14. It is possible to see that the measuring points set on the left side of the plate are cooled by a higher flow rate than the ones set on the right. As previously said, by having higher flow rate, more water is impinged toward the plate, and therefore, more cooling takes place, reporting lower temperature values. This difference is less highlighted over the surface of the plate, while the deeper the measure takes place, the more outstanding it is.

It is possible to calculate temperature drop rate to achieve an overall picture of quenching heat transfer footprint along the measurement line in time close to the quenched surface. Therefore, cooling rate can be calculated by the following equation,

$$\frac{dT}{dt} = \frac{T_{t+\Delta t} - T_t}{\Delta t} \left[ \frac{^{\circ}\text{C}}{\text{s}} \right] \quad (5.1)$$

where  $\Delta t$  is frequency of temperature measurement (50 Hz), and  $T_{t+\Delta t}$  is the temperature recorded one time step after  $T_t$ . The 3-D plot of cooling rate is shown in Figure 15 shows clearly that larger flow rate in the jet in  $X = 0 \text{ mm}$  provided higher cooling rate compare to the other stagnation region around  $X = 50 \text{ mm}$ . It also shows clearly that the cooling rate in the upwash zone ( $X = 25 \text{ mm}$ ) is very poor in the beginning of quenching and after wall water jets collide to each other after some time (about 5.5 s), cooling rate is increased in the upwash region as well. Similar footprint of heat transfer is expected in the quenched surface with much larger cooling rate values.

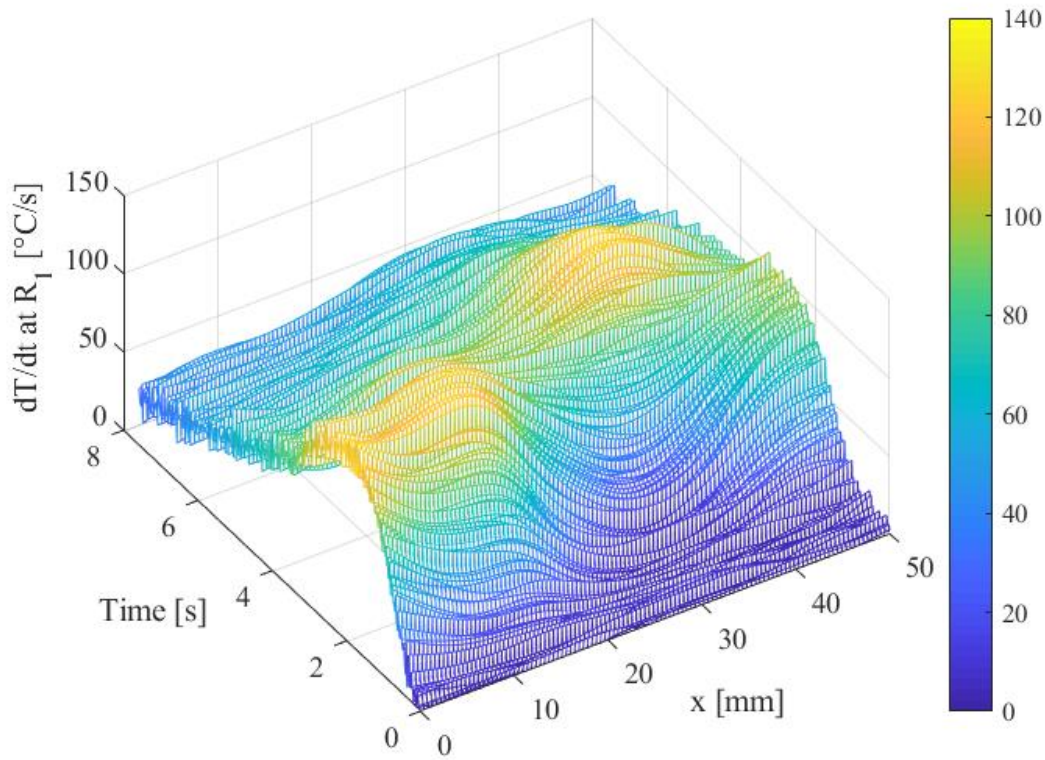


Figure 15: Cooling rate ( $\frac{dT}{dt}$ ) at line  $R_1$ , Test 5

### 5.1 Effect of velocity

From previous researches and experiments, it was concluded that higher jet velocity led to higher cooling rate. In tests 1, 4 and 5, the velocity parameter is varied, taking the values of 1.9, 2.9 and 3.9 m/s. From these experiments, a comparison of temperature distribution along the plate at time  $t = 3$  seconds after beginning of quenching has been made, as it can be seen in Figure 16 and Figure 17. It may be easy to notice that lower temperatures are reached along the line with higher jet velocities, which ultimately means higher cooling rates. The overall shapes of the curves hint that the upwash flow point has been moved to the right,  $X \approx 30$  mm, since higher velocities with the same nozzle area brings higher flow rates and wall jet velocity. Therefore, higher wall jet velocity of water jet in  $X=0$  mm will push the wall jet from adjacent jet in  $X=50$  mm and upwash flow position is moved slightly to  $X \approx 30$  mm. Clearly, Figure 16 presents higher values of temperature compared to Figure 17, for heat transfer phenomenon is more dominant as being closer to the surface.

It may be eye-catching that in Figure 16, a striking crossing takes place on the right side between  $U = 2.9$  m/s curve and  $U = 3.9$  m/s curve. This is due to a very small difference

in starting delay time in pump 2, which eventually begins cooling with small delay in those points. With this in mind, it is easy to realize that  $U = 2.9$  m/s curve would keep a similar trend as the others from  $X \approx 25$  mm on.

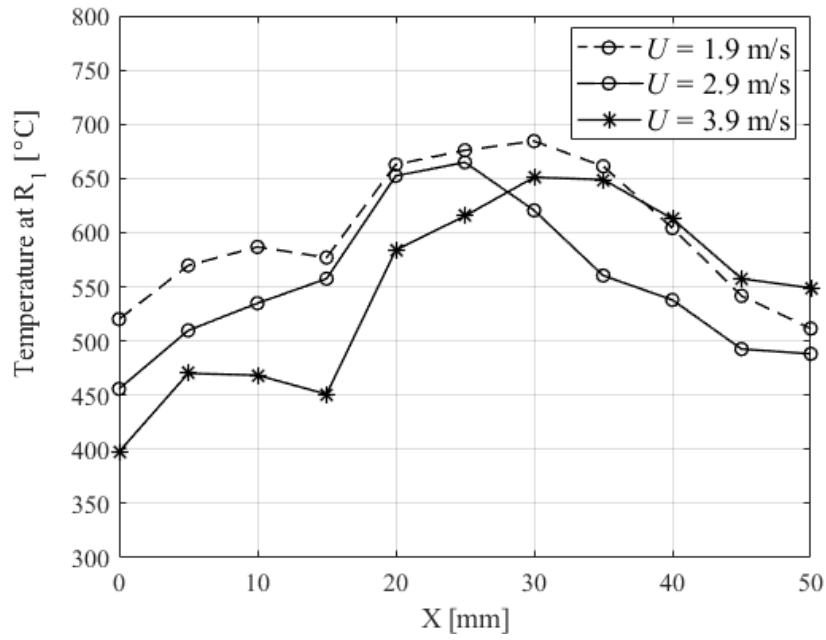


Figure 16: Effect of jet velocity on temperature distribution at  $R_1$

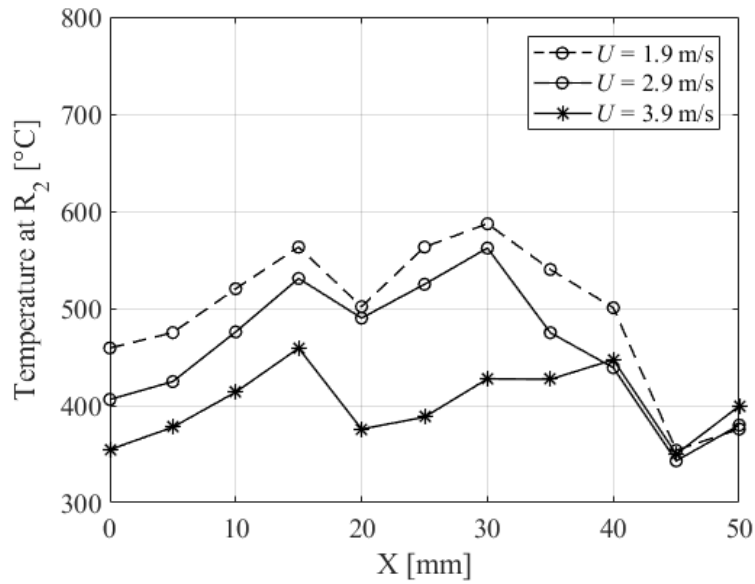


Figure 17: Effect of jet velocity on temperature distribution at  $R_2$

## 5.2 Effect of jet diameter

In experiments 1, 2 and 3, influence of jet diameter over quenching is analysed. It is convenient to point out, that although the size of the nozzle is varied, the flow rate is not. This means that the latter is kept constant throughout the experiments, which leads to a simultaneous variation of the velocity parameter, but with no shifting of the upwash flow point. That said, it is right to mention that these results present a behaviour relation between jet diameter and jet velocity. By looking at Figure 18 and Figure 19, it is safe to state that no special relevance lies upon this parameter if no flow rate variation exists. The three curves of various  $d$  present same trend, and the effects they may have on improving cooling rate are negligible. Only slightly better cooling is achieved by  $d = 4$  mm as the jet velocity is higher as well in this test.

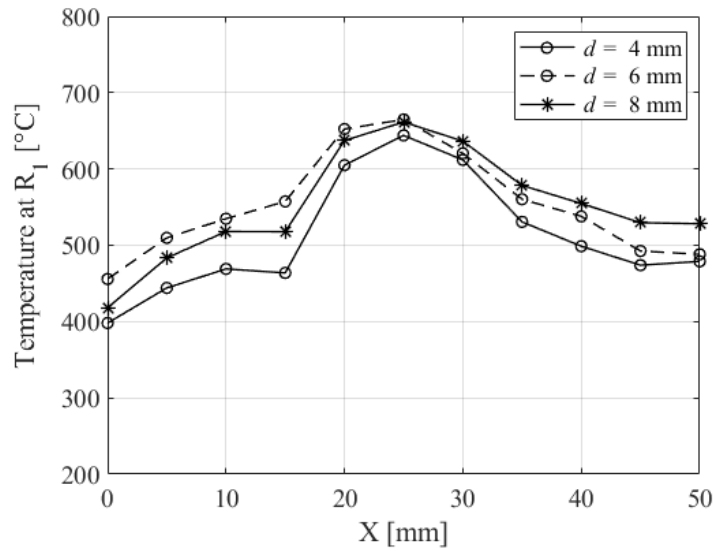


Figure 18: Effect of jet diameter on temperature distribution at  $R_1$

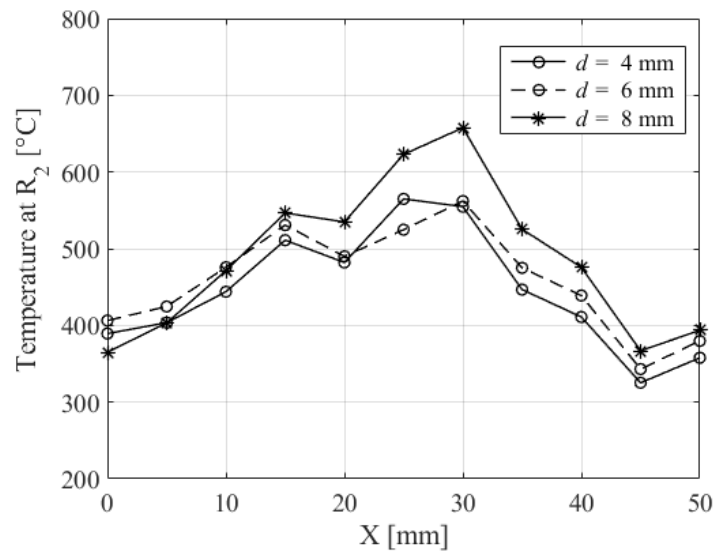


Figure 19: Effect of jet diameter on temperature distribution at  $R_2$

### 5.3 Effect of initial quenching temperature

The initial temperature is a parameter which holds more meaning than it may seem at first. As it may be seen in Figure 20 and Figure 21, from tests 1, 6, 7 and 8, the lower the initial temperature, the lower the temperature distribution along the plate. This may sound obvious, but no hint is given in terms of cooling rate. If initial temperature takes high values, different boiling regimes appear during quenching, and therefore the cooling rate varies greatly along the process. From previous studies it was said that  $q_s''$  achieves higher values during nucleate boiling, which usually takes place at low values of  $\Delta T_e$ . If the sample is taken to high values of temperature, film boiling will occur, and low  $q_s''$  values will be reported. Formation of vapor bubbles, and thus the vapor layer, avoids liquid-solid contact, which results in lower heat extraction from the sample. On the other hand, the upwash flow point is not affected by this parameter, since its dependence is mainly to the flow rate, and no variation of it is found in this experiment.

When analysing the information showed in the graphs, it is important to keep in mind that some small start delays may appear on the water pumps performance. These delays might lead to different temperature values compared to the ones there should truly appear. In this case, a start delay on pump 1 results in lower values of temperature reported by the sensors placed on the right end on the measuring line. Since pump 2 has had the chance to start quenching sooner than pump 1, more cooling will be shown on one side than the other for a specific measuring time.

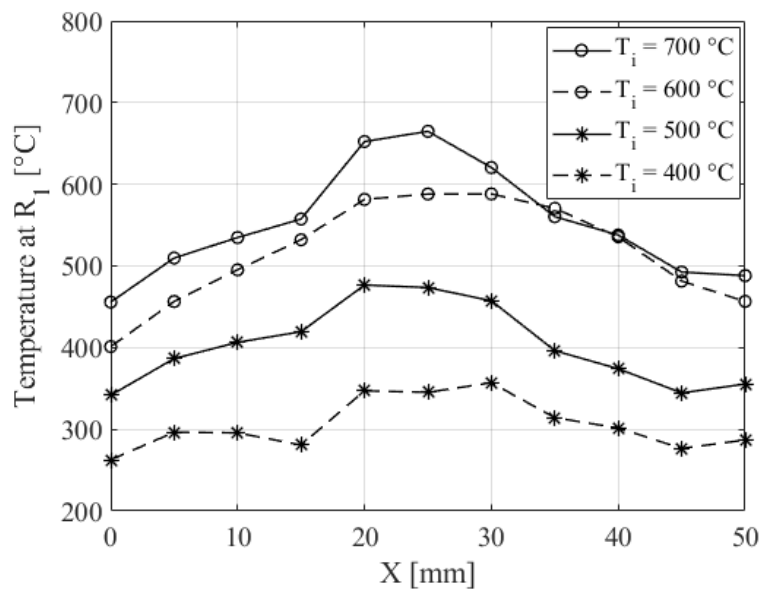


Figure 20: Effect of initial temperature on temperature distribution at  $R_1$



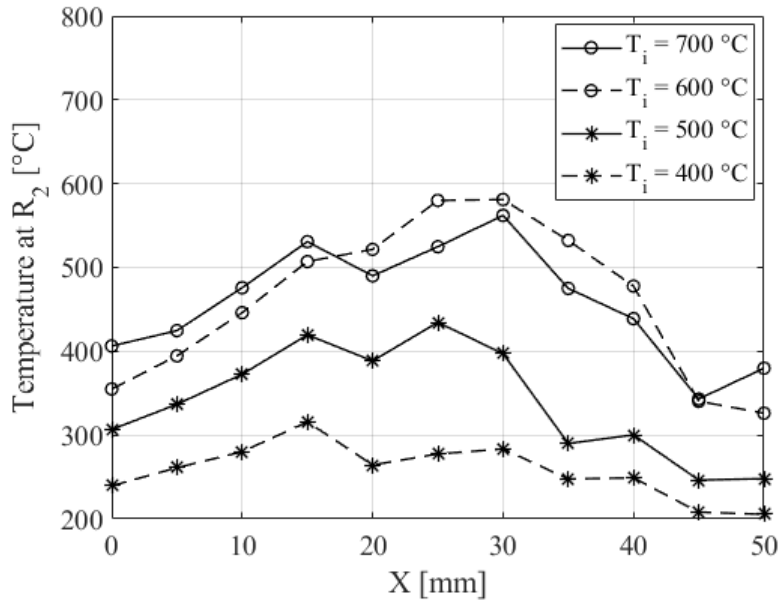


Figure 21: Effect of initial temperature on temperature distribution at  $R_2$

It is possible to compare the cooling rate footprint of tests with different initial quenching temperature in order to obtain the overall effect of  $T_i$  on quenching process. As it can be seen in Figure 22, similar variation of cooling rate is seen along the experiments while the magnitude of cooling rates decreases slightly by reducing initial quenching temperature. It is also interesting that upwash flow region's cooling rate is not pronounced strongly in tests  $T_i=700^{\circ}\text{C}$ , while the upwash flow peak value is clear in the experiments with lower  $T_i$ . This phenomenon may be due to existence of both film and transition boiling regime in the test  $T_i=700^{\circ}\text{C}$ , which damps the cooling in the upwash flow region.

On the other hand, the position of upwash flow point is not affected by initial quenching temperature, and no variation is found in this experiment.

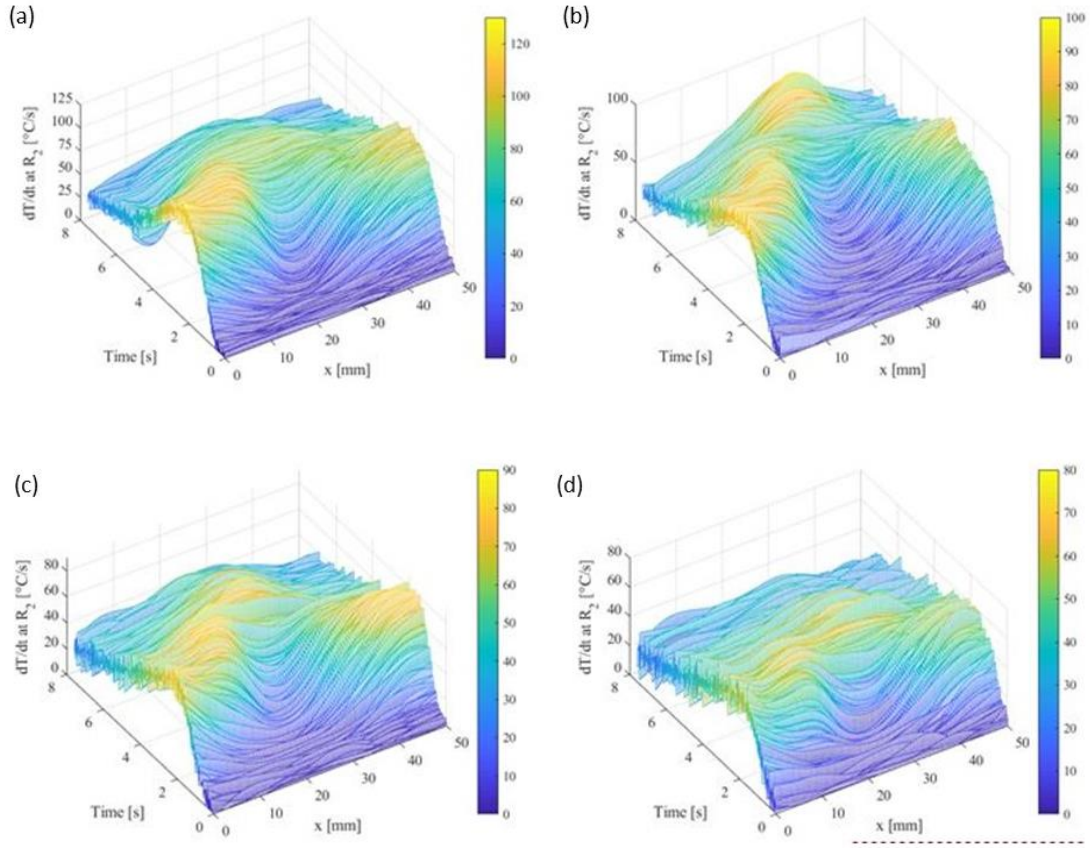


Figure 22: 3-D contour plots of cooling rate in tests (a)  $T_i=700^\circ\text{C}$ , (b)  $T_i=600^\circ\text{C}$ , (c)  $T_i=500^\circ\text{C}$ , (d)  $T_i=400^\circ\text{C}$ .

## 5.4 Effect of subcooling

Subcooling temperature, expressed by  $\Delta T_{sub}$ , was defined as the difference between  $T_{sat}$  and fluid temperature. By analysing the results obtained from Test 1 and 9, and showed in Figure 23 and Figure 24, two ideas may be extracted: On the one hand, the upwash flow point is not affected by this parameter. No shifting of the point is performed, since there is no change in the cooling rate. On the other hand, the higher the value of  $\Delta T_{sub}$ , which means lower fluid temperature, the lower the temperature measured on the points, and therefore higher cooling rates.

Having a look on the graphs, it is possible to realize there exists again a delay start on pump 1. The reason of this is not only given by the crossing between the two curves, but also because it is known that the pump 2, which is in charge of cooling the right end of the measuring line, presents a flow rate lower than the one held by pump 1, that would lead to lower cooling rates and therefore higher temperature values than the ones on the left end.

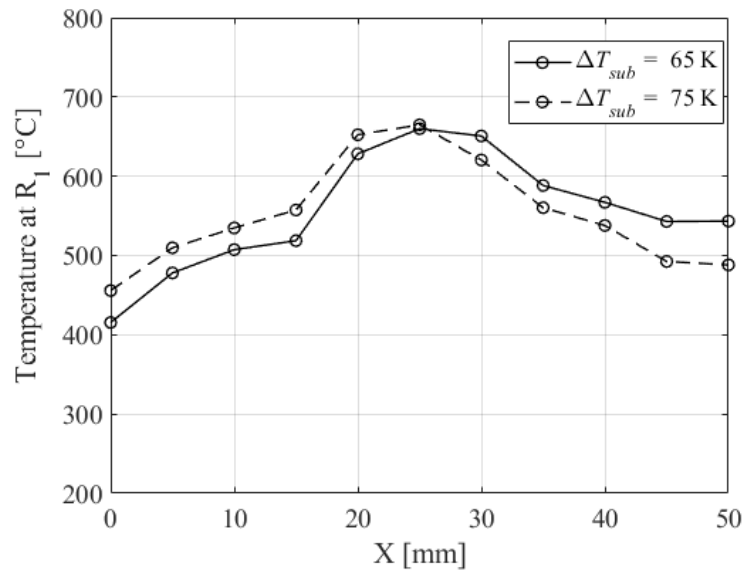


Figure 23: Effect of subcooling on temperature distribution at  $R_1$

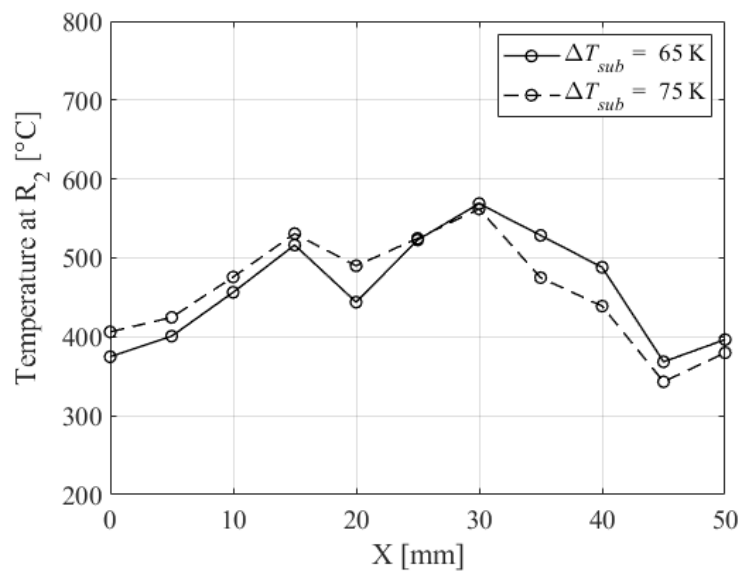


Figure 24: Effect of subcooling on temperature distribution at  $R_2$

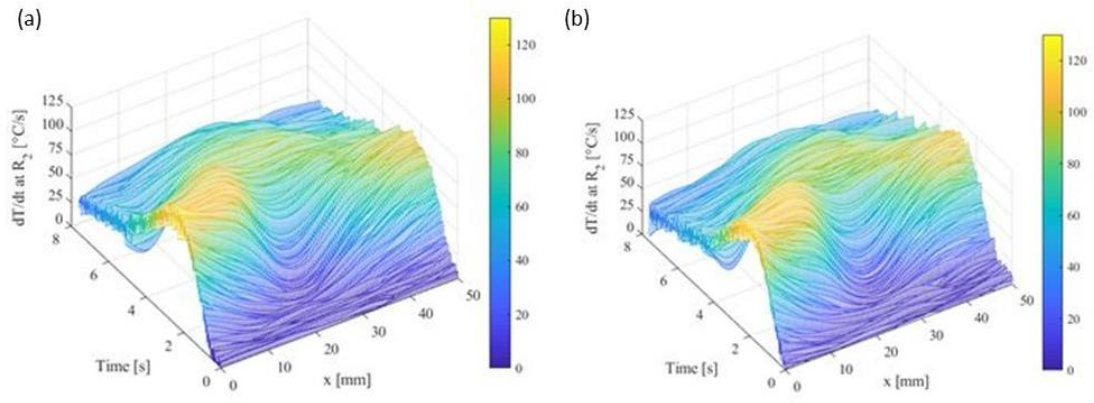


Figure 25: 3-D contour plots of experiments with different subcooling temperature (a)  $\Delta T_{sub} = 75\text{K}$ , (b)  $\Delta T_{sub} = 65\text{K}$

## 6. Conclusions

The aim of this master thesis was to study quenching a heated plate by multiple configuration of water impinging jets on a heated plate. Two different flow rates are introduced simultaneously in each experiment in the quenching of two cooling area over the steel plate, to examine the possibility of producing various cooling rates over the total steel plate surface on a heated plate. This can lead to development of various material properties in the material in small areas for specific applications.

The study has been focused on several parameters which have been varied as different flow rates were used simultaneously to cool down different parts of the plate.

### 6.1 Study results

After running the different parametric study described, next ideas are extracted:

- The higher the water jet velocity used in quenching, the lower the temperature of the plate, and therefore the higher the cooling rate achieved. Since the flow rate of jets in  $X = 50$  mm was constant, greater difference between flow rate of water jets on  $X = 0$  and 50 mm provided more pronounced cooling rate differences over the steel plate.
- The jet diameter has no substantial effect on varying the cooling rate if the flow rate is kept constant. The variation of this parameter only has a positive in quenching if it originates higher flow rates, which ultimately produces a higher cooling rate.
- With initial quenching temperature of 600 and 700°C, higher cooling rate is obtained in the stagnation region of jets, and no significant changes on the difference of cooling rates at two ends of plate were observed. Upwash flow's peak cooling rate is more pronounced at lower initial quenching temperature.
- The higher the subcooling, the lower the fluid temperature used for quenching, and therefore the higher the cooling rate. The heat extraction potential turns higher if more heat energy gap is presented between the fluid and solid. Nevertheless, the differences in the cooling rate are not significant in the tested range of subcooling in this study.
- The shifting of the upwash flow point from its original position in the middle of measurement line ( $X = 25$  mm) is only caused by the flow rate difference between the jets. If the flow rate of one pump is much higher than the other one, the strength of the first will push the upwash flow point to the opposite end.

## 6.2 Outlook

This study is described as experimental, and because of it, performing errors, measurement imbalances and other inaccuracies may come up. All these details and more have been detected, analysed and considered if necessary, so nothing is left to chance. But these limitations and setbacks the study presents, either by the equipment used or by the assumptions made, open the door to new ways of improving this type of experiments and creating new avenues of thought.

The ideas and statements reported by the results have agreed with previous experiments and researches, and it has also been proved that it is possible to work with different flow rates without disrupting each other's performance, obtaining different cooling rate levels on diverse areas. This situation may contribute to different material properties in the steel sample, bringing up the possibility of carrying out different quenching processes at the same time, saving both time and money.

Yet, the study about quenching is not finished. The possibilities of this technique are huge, and its understanding and comprehension are not completed. More research must be done both in the quenching technique optimization, and material properties development.

## 6.3 Perspectives

Quenching by water impinging jets is not the best example of energy production system. As explained before, it is a revolutionary technique inside the steel industry, whose aim is not orientated to achieve lower carbon emissions or reduce energy consumption, but to improve the process by reducing working times and raising efficiency. By all odds, some people have seen certain potential in using the waste heat from the return hot water. But due to the small dimensions of the steel plate, and therefore the small amount of water used during the quenching process, this heat recovery is not worth it. Therefore, the idea of studying this technique in a broader perspective, specifically in terms of sustainable development, does not entirely match with this topic.

## 7. Index of Figures

Figure 1: Temperature-time curve during quenching [1].....	4
Figure 2: Boiling curve for water at 1 atm [4]. .....	5
Figure 3: Industrial water tank used for quenching [5].....	8
Figure 4: Jet impinging jet [6] .....	9
Figure 5: Fluid flow regions of a single impinging jet [6].....	10
Figure 6: Possible fountains developed in a multi-jet configuration [7].....	11
Figure 7: Distinct regions identified on the impingement surface during quenching [10] .....	12
Figure 8: Schematic of experimental set-up.....	17
Figure 9: Schematic of nozzles and plate .....	18
Figure 10: Schematic of jet position and the drilled configuration of holes in the plate to install thermocouples in lines <i>R1</i> and <i>R2</i> . .....	19
Figure 11: Temperature-time relation of measurement line <i>R1</i> , Test 5 .....	23
Figure 12: Temperature-time relation of measurement line <i>R2</i> , Test 5 .....	24
Figure 13: Temperature distribution in line <i>R1</i> at different time steps, Test 5.....	25
Figure 14: Temperature distribution in line <i>R2</i> at different time steps, Test 5.....	25
Figure 15: Cooling rate ( $dT/dt$ ) at line <i>R1</i> , Test 5 .....	27
Figure 16: Effect of jet velocity on temperature distribution at <i>R1</i> .....	28

Figure 17: Effect of jet velocity on temperature distribution at $R2$ .....	28
Figure 18: Effect of jet diameter on temperature distribution at $R1$ .....	29
Figure 19: Effect of jet diameter on temperature distribution at $R2$ .....	29
Figure 20: Effect of initial temperature on temperature distribution at $R1$ .....	30
Figure 21: Effect of initial temperature on temperature distribution at $R2$ .....	31
Figure 22: 3-D contour plots of cooling rate in tests (a) $Ti=700^{\circ}\text{C}$ , (b) $Ti=600^{\circ}\text{C}$ , (c) $Ti=500^{\circ}\text{C}$ , (d) $Ti=400^{\circ}\text{C}$ .....	32
Figure 23: Effect of subcooling on temperature distribution at $R1$ .....	33
Figure 24: Effect of subcooling on temperature distribution at $R2$ .....	33
Figure 25: 3-D contour plots of experiments with different subcooling temperature (a) $\Delta T_{sub}=75\text{K}$ , (b) $\Delta T_{sub}=65\text{K}$ .....	34



## 8. Index of Tables

Table 1: Designed range of parameters in the experiments.....	21
Table 2: Material concentration of the sample [16]. .....	21
Table 3: List of tests in the parametric study. ....	22

## 9. References

- [1] J. Á. Pardo, "Enlace, metales y estructuras cristalinas," *Departamento de Ciencia y Tecnología de Materiales y Fluidos*. Univeridad de Zaragoza, Zaragoza.
- [2] J. M. F. G. y M. A. M. Sediles, "Temple Y Revenido," *Met. y Trat. Térmicos*, p. 164, 1999.
- [3] J. Á. Pardo, "Tratamiento térmico de los aceros," *Departamento de Ciencia y Tecnología de Materiales y Fluidos*. Univeridad de Zaragoza, Zaragoza.
- [4] T. L. Bergman, F. P. Incropera, A. S. Lavine, and D. P. Dewitt, *Fundamentals of Heat and Mass Transfer*, 7th ed. John Wiley & Sons, 2007.
- [5] Con Mech Engineer, "Water Quench & Temper," 2019. [Online]. Available: <http://www.conmecheng.com/heattreatment/services-detail.php?id=183>.
- [6] B. Weigand and S. Spring, "Multiple Jet Impingement - A Review," *Heat Transf. Res.*, vol. 42, no. 2, pp. 101–142, 2011.
- [7] M. Jahedi and B. Moshfegh, "Quenching a rotary hollow cylinder by multiple configurations of water-impinging jets," *Int. J. Heat Mass Transf.*, vol. 137, pp. 124–137, 2019.
- [8] N. Hatta and K. Hanasaki, "Numerical Analysis of Cooling Characteristics for Water Bar.," 1983.
- [9] A. K. Mozumder, Y. Mitsutake, and M. Monde, "Subcooled water jet quenching phenomena for a high temperature rotating cylinder," *Int. J. Heat Mass Transf.*, 2014.
- [10] N. Karwa, L. Schmidt, and P. Stephan, "Hydrodynamics of quenching with impinging free-surface jet," *Int. J. Heat Mass Transf.*, 2012.
- [11] M. Jahedi and B. Moshfegh, "Experimental study of quenching process on a rotating hollow cylinder by one row of impinging jets," 2017.
- [12] X. Yan and N. Saniei, "Heat transfer from an obliquely impinging circular air jet to a flat plate," *Int. J. Heat Fluid Flow*, vol. 18, no. 6, pp. 591–599, 1997.
- [13] C. Agrawal, R. Kumar, A. Gupta, and B. Chatterjee, "Effect of jet diameter on the maximum surface heat flux during quenching of hot surface," *Nucl. Eng. Des.*, vol. 265, pp. 727–736, 2013.
- [14] M. Gradeck, A. Kouachi, J. L. Borean, P. Gardin, and M. Lebouché, "Heat transfer from a hot moving cylinder impinged by a planar subcooled water jet," *Int. J. Heat Mass Transf.*, 2011.
- [15] M. A. Islam, M. Monde, P. L. Woodfield, Y. Mitsutake, and A. K. Mozumder, "Jet Impingement Boiling in Hot Surfaces Well Above the Limiting Temperature for Solid-Liquid Contact," *Multiph. Sci. Technol.*, vol. 19, no. 2, pp. 167–181, 2008.
- [16] SSAB, "SSAB Boron 27." [Online]. Available:

<https://www.ssab.es/products/brands/ssab-boron-steel/products/ssab-boron-27?accordion=downloads>.



*"I think nature's imagination is so much greater than  
man's, she's never going to let us relax"*

*Richard Feynman*

